XX IMEKO World Congress
Metrology for Green Growth
September 9–14, 2012, Busan, Republic of Korea

# REAL–TIME ESTIMATION OF DYNAMIC MULTI–DIMENSIONAL MEASURANDS

*Giampaolo E. D'Errico, Nadir Murru*

Istituto Nazionale di Ricerca Metrologica (INRIM), Torino, Italy, g.derrico@inrim.it

**Abstract:** This paper is devoted to the study and implementation of real–time techniques for the estimation of time–varying, contingently correlated quantities, and relevant uncertainty. An estimation algorithm based on a metrological customization of the Kalman filtering technique is presented, starting from a Bayesian approach. Moreover, a fuzzy–logic routine for real–time treatment of possible outliers, is incorporated in the overall software procedure. The system applicability is demonstrated by results of simulations performed on dimensional measurement models.

**Key words:** Kalman filter, real–time estimation, time–varying measurands, correlation, outlier treatment.

## 1. INTRODUCTION

In the context of in–process metrology, accurate statistical analyses are important to optimize real–time estimation of measurands and related uncertainties. The Kalman filtering technique (KF) [1] is optimal under diverse criteria [2]. Moreover, it is widely used long since and it is successfully being applied in several fields (see, e.g., [3], [4], [5]).

In [6] and [7], a novel application of Kalman filter is developed in the field of dimensional metrology. In [6], such customization is applied to coordinate measuring machines (CMMs). In [7], the measurands are vectorial quantities that can vary during time, according to some specified patterns. Some simulations are executed in order to discuss the algorithm performance. Both papers consider the measurands as unknown parameters, modeled in term of mutually independent normal random variables (RVs).

In the present paper, the model is improved by taking into account possible correlations among RVs, so to manage dependence among measurands. The problem is approached using the covariance matrix, which is an established technique in the KF (see, e.g., [8], [9], [10]). Finally, a routine is proposed to perform an outlier treatment based on fuzzy logics (applicability of fuzzy logics in uncertainty treatment is dealt with in [11]). Even if the KF is robust by design (against, e.g., initial uncertainty and round–off errors) its performance could be affected by occurrence of possible outliers [12]. In [13] a strategy, based on a fuzzy–logic approach, was proposed for possible outlier treatment. In the present paper, such a strategy is embedded in the estimation procedure.

The paper is organized as follows. Section 2 is devoted to the algorithm formulation. A metrological customization of the KF is derived starting from the Bayes theorem by using Gaussian multivariate distribution functions (MDFs) and managing correlations (if any) via Gaussian copula (subsection 2.1). The fuzzy outlier treatment presented in [13] is briefly recalled and embedded in the KF estimation algorithm (subsection 2.2). Section 3 presents the overall software (SW) architecture by means of a Simulink™, [1] diagram. In Section 4, some application examples are shown, where the estimation targets are two rectangular surfaces with a common edge. Section 5 contains some concluding remarks.

## 2. ALGORITHM FORMULATION

### 2.1 Metrological customization of Kalman filtering technique

The standard Kalman filter is a recursive technique used to estimate at each discrete time $k$ ($0 \le k \le L$, for $L$ maximum step number) the state $\mathbf{x}_k$ of a linear process described by the equation:

$$\mathbf{x}_{k+1} = A_k \mathbf{x}_k + B_k \mathbf{u}_k + \eta_k \tag{1}$$

where $\mathbf{x}_k$, $\mathbf{u}_k$ (optional control input), and $\eta_k$ (white noise) are vectors, and $A_k, B_k$ are matrices which relate the process state at the step $k+1$ with the $k$–th process state and with the $k$–th control input, respectively. The (indirect) measurement $\mathbf{z}_k$ of $\mathbf{x}_k$ is modeled as follows:

$$\mathbf{z}_k = H_k \mathbf{x}_k + \mathbf{v}_k \tag{2}$$

where $\mathbf{v}_k$ is introduced due to the measurement uncertainty and $H_k$ relates the (observable) output $\mathbf{z}_k$ with the (internal) state $\mathbf{x}_k$. In metrology terms, $\mathbf{z}_k$ and $\mathbf{x}_k$ represent the measured quantity values and the theoretical measurand, respectively. The vector $\mathbf{u}_k$ is used to track the time–evolution of the theoretical pattern of $\mathbf{x}_{k+1}$. In these terms, the model is translated into the context of measurement science. The estimation is provided balancing the measured quantity $\mathbf{z}_k$ with an a–priori estimation $\mathbf{x}_k^-$ by using the Kalman gain matrix $K_k$:

$$\mathbf{y}_k = \mathbf{x}_k^- + K_k(\mathbf{z}_k - H_k \mathbf{x}_k^-), \quad 0 \le k \le L \tag{3}$$

where $\mathbf{y}_k$ is the estimation of $\mathbf{x}_k$ provided by the KF and

$$\begin{cases} \mathbf{x}_0^- = \mathbf{y}_{-1} \\ \mathbf{x}_k^- = A_{k-1}\mathbf{y}_{k-1} + B_{k-1}\mathbf{u}_{k-1}, \quad 1 \le k \le L \end{cases} \tag{4}$$

where $\mathbf{y}_{-1}$ is an a–priori expert judgment of the measurand vector at the initial state. The gain matrix $K_k$ is constructed using the covariance matrix of the RVs relevant to the components of the vector $\mathbf{x}_k$. $K_k$ is obtained by minimizing the

[1] Identification of commercial products in this paper does not imply recommendation or endorsement, nor does it imply that the products identified are necessarily the best available for the purpose

mean–square–error $E[(\mathbf{y}_k - \mathbf{y}_k)(\mathbf{y}_k - \mathbf{x}_k)^T]$ where $E[\cdot]$ stands for expectation and superscript $T$ for transposition.

In [6], the KF technique has been customized for metrology usage, dealing with scalar time–invariant quantities. In [7], such an approach has been generalized to time–varying measurand vectors, whose components were supposed mutually independent.

In the present paragraph, the approach is further developed, so to take into account possible correlations among the measurand vector components; moreover, an outlier treatment incorporated in the estimation procedure is developed in §2.2.

Let $\mathbf{X}$ and $\mathbf{Z}$ represent the stochastic counterparts of $\mathbf{x}_k^-$ and $\mathbf{z}_k$, respectively. The Kalman gain matrix $K_k$ can be derived by using the Bayes theorem:

$$f(\mathbf{X}|\mathbf{Z}) = f(\mathbf{Z}|\mathbf{X})f(\mathbf{X})\left(\int_{-\infty}^{+\infty} f(\mathbf{Z}|\mathbf{X})f(\mathbf{X})d\mathbf{X}\right)^{-1} \quad (5)$$

where $f$ is a probability density function (PDF), $f(\mathbf{X}|\mathbf{Z})$ is the posterior density, $f(\mathbf{X})$ is the prior density, $f(\mathbf{Z}|\mathbf{X})$ is the likelihood, and the denominator is a normalization factor.

The following treatment will be based on the hypothesis of Gaussian RVs to model the vector measurands. In order to manage possible correlations, the Gaussian copula is a useful tool to obtain Gaussian MDFs from any vector of univariate cumulative distribution functions (CDFs): a copula is a function that couples univariate (marginal) cumulative distributions into a joint MDF, whose expression includes original correlations among marginal univariates [14].

Let $\mathcal{N}(\mu,\Sigma)$ denote a Gaussian MDF, where $\mu$ is the vector of mean values and $\Sigma$ is the covariance matrix. A Gaussian copula $C$ is a particular family of copulas such that, given $n$ marginals $h_1,...,h_n$:

$$C(h_1,...,h_n) = G_\Sigma(g^{-1}(h_1),...,g^{-1}(h_n)) = \mathcal{N}(\mu,\Sigma)$$

where $G_\Sigma$ is the $n$–variate Gaussian CDF with covariance matrix $\Sigma$ and $g$ is the univariate standard Gaussian.

Let $f(\mathbf{X}) = \mathcal{N}(\mathbf{x}_k^-, P_{k-1})$, $f(\mathbf{Z}|\mathbf{X}) = \mathcal{N}(\mathbf{z}_k, R)$ and

$$\begin{cases} P_{-1} = \tilde{P}_{-1} \\ P_k = (P_{k-1}^{-1} + R^{-1})^{-1}, \quad 0 \le k \le L \end{cases} \quad (6)$$

with $\tilde{P}_{-1}$ and $R$ symmetric covariance matrices initialized according to prior knowledge (based on an expert judgment): diagonal entries can be used for type B uncertainty treatment (see guide [15]) and other non–zero entries represent mutual correlation coefficients. Eq. (5) reads

$$f(\mathbf{X}|\mathbf{Z}) \propto \mathcal{N}(\mathbf{x}_k^-, P_{k-1})\mathcal{N}(\mathbf{z}_k, R) = \mathcal{N}(\mathbf{y}_k, P_k)$$

where

$$\mathbf{y}_k = (P_{k-1}^{-1} + R^{-1})^{-1}(P_{k-1}^{-1}\mathbf{x}_k^- + R^{-1}\mathbf{z}_k), \quad 0 \le k \le L \quad (7)$$

The final estimates are provided in terms of $E(f(\mathbf{X}|\mathbf{Z}))$ together with standard uncertainty (after square roots of diagonal entries from the covariance matrix) evaluated at $k = L$ (see [7], [19]). Equations (4), (6), (7) form the recursive algorithm used in this paper for KF metrological customization.

### 2.2 Fuzzy logic–based modeling of outlier detection and treatment

The algorithm is enriched by a routine for real–time treatment of possible outliers, that can affect the estimation results. Several statistical tests have been proposed to manage this problem, such as Dixon's test and Grubbs' one: a standard also deals with such a problem [16]. However, tests of orthodox statistics kind — beside being prone to Bayesian criticism — are also subject to statistical hypotheses, mainly randomness and independence of observations [17], [18], that impose applicability limitation in order to preserve consistency.

In [13] a fuzzy approach is proposed aiming at coping with this situation, by modeling the problem of outliers in terms of fuzzy sets, so to treat the processed observations by means of purposely defined outlierness degrees.

The fuzzy strategy, based on a 2–input/1–output inference scheme [13], operates as follows. Let $z$ be a measurand observation, $\eta$ an a–priori estimation of the measurand, $\sigma$ the a–priori estimation uncertainty, and let the distance $d(z,\eta)$ and the percentage uncertainty $\bar{\sigma}$ be defined by $d(z,\eta) = |z-\eta|$ and $\bar{\sigma} = 100\sigma/\eta$.

In the inference scheme (Mamdani model [20] and [21]), one input is the fuzzyfication of $d(z,\eta)$ and the other input is the fuzzyfication of $\bar{\sigma}$, obtained by properly defined fuzzy sets and related membership functions (see [13] for details). The output is the outlierness degree $0 \le \rho(z) \le 1$ relative to the possible outlying observation $z$, which is obtained by application of the centroid defuzzification method (ten composition rules are used after [13]). The fuzzy treatment is activated if the condition $2\sigma < d(z,\eta) < 5\sigma$ is satisfied, otherwise: if $d(z,\eta) \le 2\sigma$, $z$ is defined a 'fully inlier' ($\rho(z) = 0$); else, if $d(z,\eta) \ge 5\sigma$, $z$ is a 'fully outlier' ($\rho(z) = 1$). After this, for estimation purpose, the outlierness degree is conveniently translated into an outlierness weight $w(z) = 1 - \rho(z)$.

In the present paper — moving from mono–dimensional (the case–study in [13]) to multi–dimensional measurands — this kind of weight is used for estimation of time–varying vector quantities after integration in the KF routine.

In the KF routine described in the previous subsection, at the step $k$, the vector $\mathbf{z}_k$ is the measurand observation, $\mathbf{x}_k^-$ is the a–priori measurand estimation, and $P_{k-1}$ is the covariance matrix elaborated to deduce the uncertainty related to $\mathbf{x}_k^-$. To apply the outlier fuzzy treatment to vectorial quantities, a component wise treatment can be performed. For every $i = 1,..,m$ (where $m$ is the measurand vector dimension), let $z_k(i)$ and $x_k^-(i)$ be the $i$–th component of $\mathbf{z}_k$ and $\mathbf{x}_k^-$ respectively, and let $P_{k-1}(i,i)$ be the $i$–th diagonal entry of the matrix $P_{k-1}$. The outlier fuzzy treatment is embedded in the KF by use of $z = z_k(i)$, $\eta = x_k^-(i)$, $\sigma = \sqrt{P_{k-1}(i,i)}$.

For the measurement vector $\mathbf{z}_k$, an outlierness weight $w_k(i)$ is associated to the measurement $z_k(i)$, giving rise to the outlierness weight vector $\mathbf{w}_k = (w_k(1),...,w_k(m))$. After evaluation, the weight $\mathbf{w}_k$ must be incorporated in the KF routine. Equation (7) that provides the estimation $\mathbf{y}_k$ in terms of

a weighted mean of $\mathbf{x}_k^-$ and $\mathbf{z}_k$ can be rewritten

$$\mathbf{y}_k = (P_{k-1}^{-1}\mathbf{x}_k^- + R^{-1}\mathbf{z}_k)(P_{k-1}^{-1} + R^{-1})^{-1}$$

making clear that $R^{-1}$ is the weight matrix of $\mathbf{z}_k$ ($R$ and its inverse $R^{-1}$ are diagonal matrices, i.e., mutual independence of measurement vector components is assumed).

For fuzzy treatment purpose, $R^{-1}$ must be scaled in terms of a diagonal matrix $Q$, to take into account $\mathbf{w}_k$ as follows:

$$Q(i,i) = R^{-1}(i,i)w_k(i), \quad \forall i = 1,...,m \tag{8}$$

Therefore, the measurand estimation in the KF is given by

$$\mathbf{y}_k = (P_{k-1}^{-1} + Q)^{-1}(P_{k-1}^{-1}\mathbf{x}_k^- + Q\mathbf{z}_k), \quad 0 \le k \le L \tag{9}$$

## 3. SOFTWARE ARCHITECTURE

The algorithm developed in Section 2 has been implemented to simulate real–time estimation of multi–dimensional time–varying measurands. The realized SW architecture is illustrated in Figure 1 by means of a Simulink$^{TM}$ diagram.

In the implemented SW procedure, the measurands are time–varying quantities, which are supposed to evolve according to patterns specified through the input 'Pattern tag' in the diagram. The possible patterns so far available are linear, sawtooth, triangular wave, square wave, sine wave, exponential and parabolic shapes, [7]. The inputs $\mathbf{y}_{-1}$, $P_{-1}$, and $R$ must be pre–set by an expert operator to initialize the routine.

At each step $k$ the routine operates as depicted in Figure 1a. The routine is fed by a measurement $\mathbf{z}_k$. The vector $\mathbf{x}_k^-$ is evaluated putting in Eq. (4) $A_{k-1} = B_{k-1} = I$ ($I$ identity matrix); $\mathbf{u}_{k-1}$ is built in the 'u evaluation' block according to the selected pattern: in Figure 1b, an example (for the exponential shape) is shown. In the 'P update' block (Figure 1c), the matrix $P_{k-1}$ is evaluated according to Eq. (6); $P_k$ is then used to compute the standard deviations $\sqrt{P_k(i,i)}$. The matrix $R$ is transformed into $Q$ ('R update' block in Figure 1d), see Eq. (8); $\mathbf{w}_k$ is evaluated in the block 'weight evaluation (fuzzy outlier treatment)' (see subsection 2.2). Finally, Eq. (9) is implemented in the 'compute estimates' (Figure 1e) block whose output provides the measurand estimation $\mathbf{y}_k$.

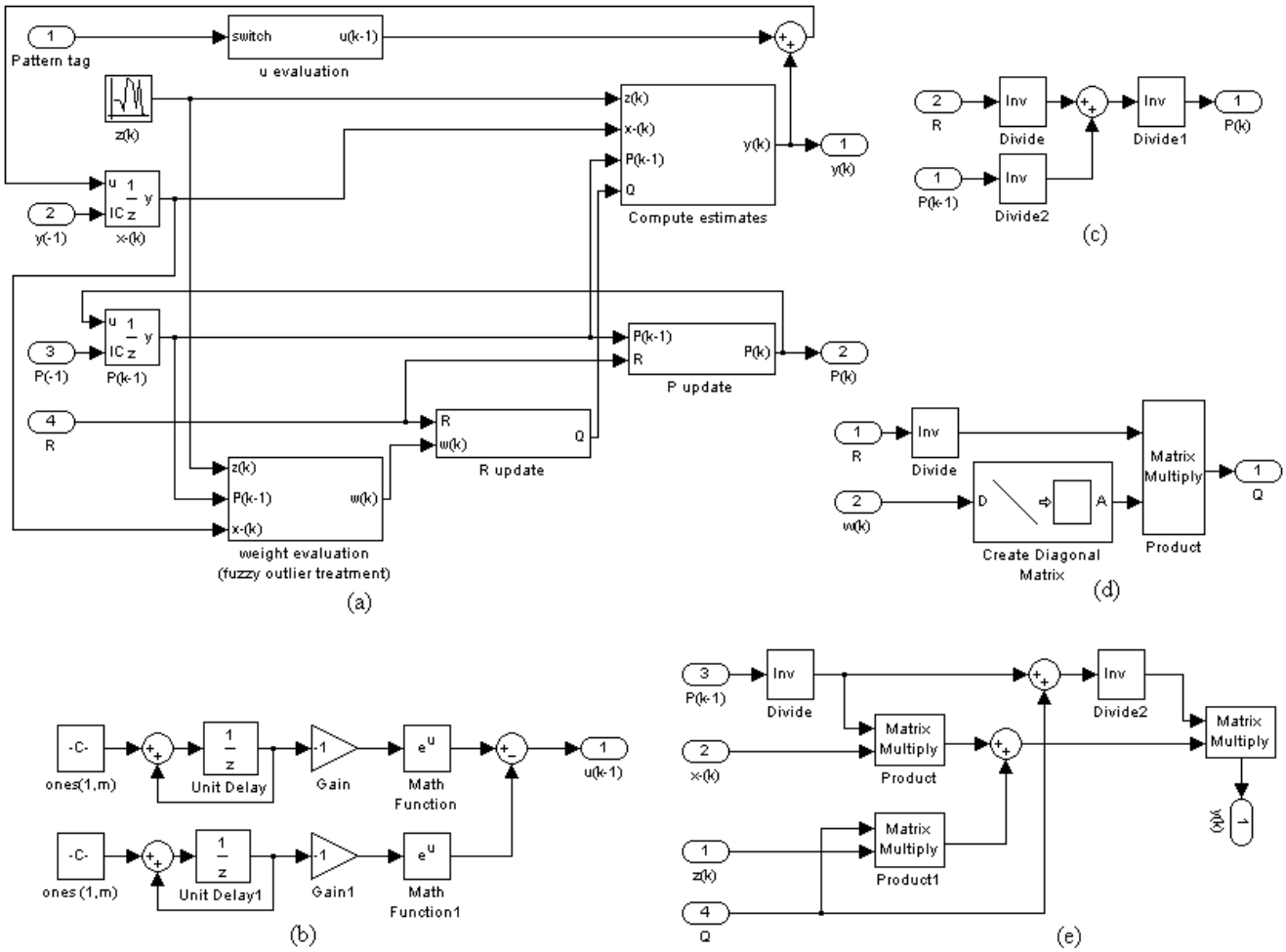


Figure 1: Simulink diagram (a) and blocks: '$u$ evaluation' (b); '$P$ update' (c); '$R$ update' (d); 'compute estimates' (e).

## 4. SIMULATION: A CASE–STUDY

The algorithm behavior is presented and discussed with application to some simulations performed in MATLAB$^{TM}$. The SW system performance is tested on a case–study where measurands are the areas of two rectangular surfaces $S1$ and $S2$ with a common edge $x3$ (Figure 2): use of $x3$ to calculate both areas introduces correlations between the components of the measurand vector $(S1, S2)$.

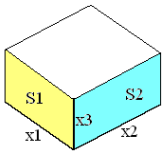


Figure 2. Rectangular surfaces $S1$ and $S2$ (measurands).

Since $S_1 = \frac{x1}{x2} S2$, it seems that a linear correlation (Pearson coefficient) can properly describe such a model. However, taking into account randomness, the routine is able to process also different correlations (Spearman and Kendall coefficients), which can be entered in the non–diagonal entries of $P_{-1}$ by an expert operator.

Measurements of $x1$, $x2$, $x3$ are modeled by independent RVs and the measurement vector $\mathbf{z}_k$ is (indirectly) obtained by $S1 = x1x3$ and $S2 = x2x3$. While $x3$ is supposed a non–varying quantity for the seek of simplicity, $x1$ and $x2$ are supposed time–varying quantities due to, e.g., temperature fluctuations: $S1$ and $S2$ follow the same patterns of $x1$ and $x2$, respectively.

Figures 3 and 4 (whose simulation data are contained in Table 1 and 2, respectively) show the algorithm behavior without outlier treatment. Figures 3a and 4a represent the first component of the measurand vector (surface $S1$) time–varying with sine and linear pattern, respectively. Figures 3b and 4b represent the second component (surface $S2$), which follows a square wave and an exponential shape pattern, respectively.

For simulation purpose, measurements of $x1$, $x2$, and $x3$ are obtained at each step by random generators, as follows: in Figure 3, $x1$, $x2$, and $x3$ are sampled from normal marginal distributions and Pearson coefficient has been used; in Figure 4 (with Kendall coefficient), $x1$ and $x2$ are obtained from uniform marginal distributions, for $x3$ a gamma marginal distribution has been used. In Figure 3: $P_{-1} = \begin{pmatrix} 0.40 & 0.43 \\ 0.43 & 0.40 \end{pmatrix}$, $R = \begin{pmatrix} 0.5 & 0 \\ 0 & 0.5 \end{pmatrix}$. In Figure 4: $P_{-1} = \begin{pmatrix} 0.85 & 0.39 \\ 0.39 & 0.75 \end{pmatrix}$, $R = \begin{pmatrix} 0.35 & 0 \\ 0 & 0.25 \end{pmatrix}$. Uncertainties relative to prior estimate and measurements are close to each other in the case of Figure 3, while in Figure 4, measurements uncertainty is less than that of prior estimate. Activation of the fuzzy outlier treatment is recommended when measurement uncertainty is significantly greater than prior estimate uncertainty: for this reason it is not activated in the simulations reported in Figures 3 and 4.

In these simulations, the algorithm is convergent and efficient, so that most estimated values are closer than measured ones and prior knowledge to the theoretical measurand pattern.

In Figure 5 (see Table 3 for data), measurements uncertainty is as large as required to activate the fuzzy outlier treatment in the KF routine. The criterion for outlier detection is based on matching $\mathbf{z}_k$ against $\mathbf{x}_k^-$: thus a majority of outlying values may result during a simulation, as in Figures 5c and 5d. Measurements are obtained by use of normal random functions and the Spearman coefficient describes correlations between $S1$ and $S2$; moreover $P_{-1} = \begin{pmatrix} 0.30 & 0.94 \\ 0.94 & 0.20 \end{pmatrix}$, $R = \begin{pmatrix} 0.9 & 0 \\ 0 & 1 \end{pmatrix}$.

A comparison between the algorithm performance with and without outlier treatment is shown in the panels of Figure 5. Figure 5a (surface $S1$, linear pattern) and Figure 5b (surface $S2$, triangular wave) display the algorithm trend when the treatment is off. In Figure 5c (surface $S1$, linear pattern) and Figure 5d (surface $S2$, triangular wave), the treatment is on. Comparing Figure 5a and 5c, it can be noted that at $k = 1, 2, 5, 8$ the effect of outlierness weights is to maintain the estimates in Figure 5c closer to the theoretical measurand. Similarly, by contrasting Figure 5b and 5d at $k = 8, 9$, a better performance can be noted in Figure 5d.

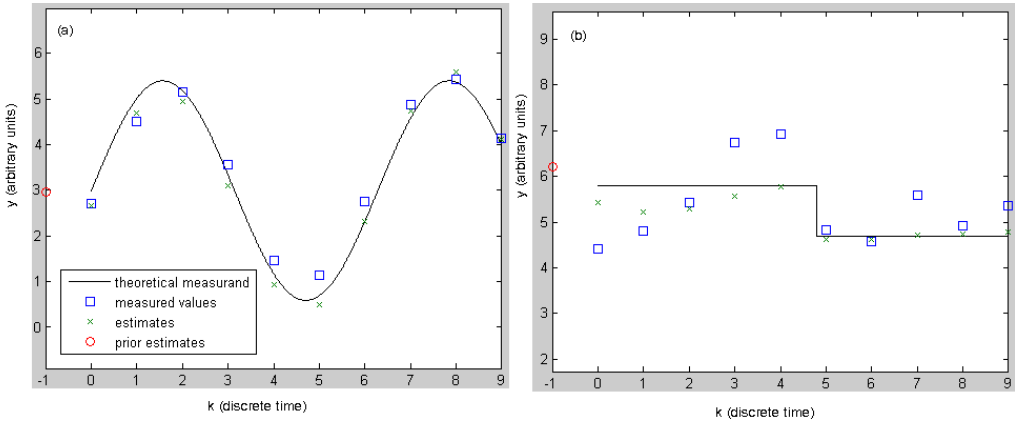


Figure 3. Cyclic patterns for $S1$ (left) and $S2$ (right): simulation results.

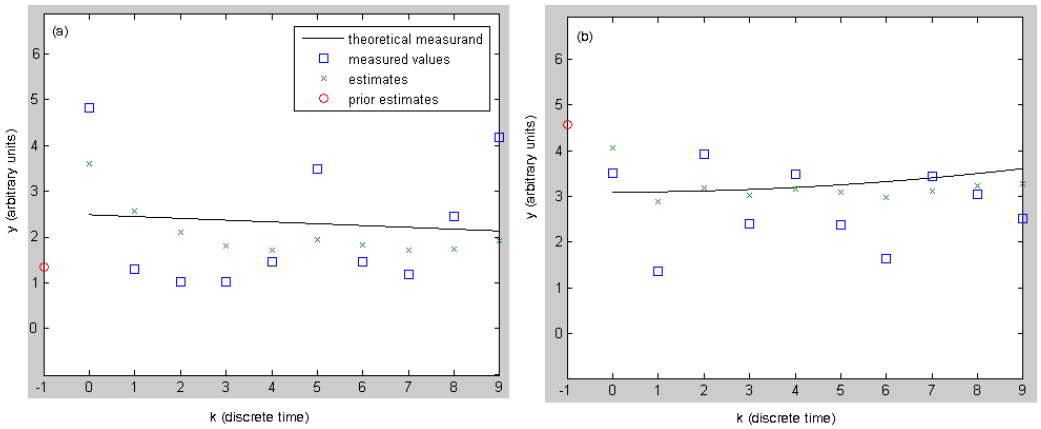


Figure 4. Acyclic patterns for $S1$ (left) and $S2$ (right): simulation results.

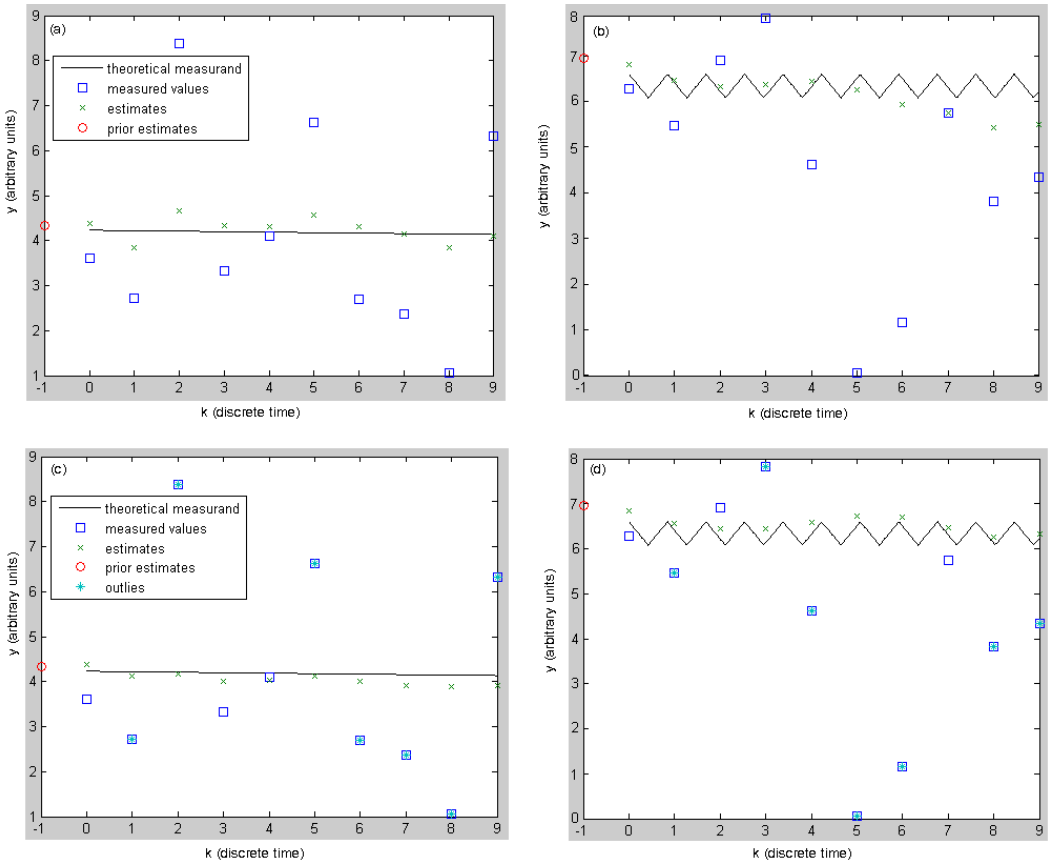


Figure 5. Comparison between KF routine with fuzzy outlier treatment off (top panels) or on (bottom).

**Table 1**. Measured (**z**), theoretical (**x**), and estimated (**y**) vectors of Figure 3.

| | $\mathbf{y}_{-1}$=(2.97, 6.21) | | |
|---|---|---|---|
| $k$ | **z** | $x$ | $y$ |
| 0 | (2.70, 4.42) | (2.99, 5.81) | (2.66, 5.43) |
| 1 | (4.50, 4.80) | (5.02, 5.81) | (4.69, 5.22) |
| 2 | (5.16, 5.43) | (5.18, 5.81) | (4.94, 5.28) |
| 3 | (3.57, 6.74) | (3.33, 5.81) | (3.11, 5.56) |
| 4 | (1.46, 6.92) | (1.17, 5.81) | (0.92, 5.78) |
| 5 | (1.24, 4.83) | (0.69, 4.87) | (0.50, 4.62) |
| 6 | (2.76, 4.57) | (2.32, 4.87) | (2.31, 4.62) |
| 7 | (4.88, 5.60) | (4.57, 4.87) | (4.74, 4.72) |
| 8 | (5.43, 4.92) | (5.37, 4.87) | (5.58, 4.74) |
| 9 | (4.14, 5.36) | (3.98, 4.87) | (4.10, 4.79) |

**Table 2**. Measured (**z**), theoretical (**x**), and estimated (**y**) vectors of Figure 4.

| | $\mathbf{y}_{-1}$=(1.35, 4.56) | | |
|---|---|---|---|
| $k$ | **z** | $x$ | $y$ |
| 0 | (4.83, 3.51) | (2.49, 3.09) | (3.62, 4.05) |
| 1 | (1.30, 1.36) | (2.45, 3.10) | (2.55, 2.87) |
| 2 | (1.02, 3.92) | (2.41, 3.12) | (2.10, 3.18) |
| 3 | (1.02, 2.40) | (2.37, 3.15) | (1.81, 3.02) |
| 4 | (1.46, 3.49) | (2.33, 3.19) | (1.71, 3.15) |
| 5 | (3.50, 2.38) | (2.29, 3.25) | (1.94, 3.10) |
| 6 | (1.46, 1.63) | (2.25, 3.32) | (1.82, 2.97) |
| 7 | (1.17, 3.43) | (2.21, 3.40) | (1.70, 3.12) |
| 8 | (2.44, 3.04) | (2.17, 3.50) | (1.74, 3.22) |
| 9 | (4.18, 2.51) | (2.13, 3.60) | (1.92, 3.28) |

**Table 3**. Measured (**z**), theoretical (**x**), and weight (**w**) vectors of Figure 5; estimated vectors (**y**) of Figures 5a and 5b; estimated vectors (**y**$^*$) of Figures 5c and 5d.

| | $\mathbf{y}_{-1}$=(4.33, 6.95) | | | | |
|---|---|---|---|---|---|
| $k$ | **z** | $x$ | $y$ | $y^*$ | $w$ |
| 0 | (3.61, 6.28) | (4.23, 6.60) | (4.39, 6.84) | (4.39, 6.84) | (1.00, 1.00) |
| 1 | (2.72, 5.46) | (4.22, 6.41) | (3.84, 6.45) | (4.12, 6.55) | (0.50, 0.50) |
| 2 | (8.37, 6.90) | (4.21, 6.22) | (4.66, 6.32) | (4.18, 6.44) | (0.00, 1.00) |
| 3 | (3.34, 7.83) | (4.20, 6.13) | (4.32, 6.37) | (3.40, 6.44) | (1.00, 0.50) |
| 4 | (4.10, 4.66) | (4.19, 6.32) | (4.31, 6.45) | (4.02, 6.60) | (1.00, 0.22) |
| 5 | (6.63, 0.05) | (4.18, 6.51) | (4.56, 6.25) | (4.11, 6.74) | (0.20, 0.00) |
| 6 | (2.70, 1.16) | (4.17, 6.50) | (4.32, 5.94) | (4.01, 6.70) | (0.50, 0.00) |
| 7 | (2.37, 5.74) | (4.16, 6.31) | (4.14, 5.74) | (3.90, 6.47) | (0.50, 1.00) |
| 8 | (1.06, 3.82) | (4.14, 6.12) | (3.84, 5.42) | (3.90, 6.25) | (0.00, 0.00) |
| 9 | (6.33, 4.35) | (4.13, 6.23) | (4.11, 5.50) | (3.91, 6.32) | (0.22, 0.22) |

## 5. CONCLUSION

An integrated software system for real–time estimation and candidate outlier treatment has been developed with application to time–varying multi–dimensional measurands.

- The estimation strategy implements a metrological customization of the Kalman filter technique, taking into account possible statistical correlation of measurands and related uncertainty evaluation.
- Occurrence of suspected outliers in dynamic measurements is modeled in fuzzy–logic terms for real–time detection and processing.
- The overall SW performance is tested by means of simulation results based on dimensional measurement data: system efficiency and convergency are demonstrated.


## ACKNOWLEDGMENT

The second author has been supported by an INRIM's post–doc fellowship.


# References


[1] R. E. Kalman, A new approach to linear filtering and prediction problems, Trans. ASME D, J. Basic Eng., vol. 82, pp. 35–45, 1960.

[2] H. W. Sorenson, Least–squares estimation: from Gauss to Kalman, IEEE Spectrum, vol. 7, no. 7, pp. 63–68, 1970.

[3] C. Mitsantisuk, S. Katsura and K. Ohishi, Kalman–filter–based sensor integration of variable power assist control based on human stiffness estimation, IEEE Trans. Ind. Electron., vol. 56, no. 10, pp. 3897–3905, 2009.

[4] N. Salvatore, A. Caponio, F. Neri, S. Stasi, and G. L. Cascella, Optimization of delayed–state Kalman–filter–based algorithm via differential evolution for sensorless control of induction motors, IEEE Trans. Ind. Electron., vol. 57, no. 1, pp. 385–394, 2010.

[5] W. L. Chan, C. S. Lee, and F. B. Hsiao, Real–time approaches to the estimation of local wind velocity for a fixed–wing unmanned air vehicle, Meas. Sci. Technol., vol. 22, no. 105203 (10pp), doi: 10.1088/0957-0233/22/10/105203, 2011.

[6] G. E. D'Errico, Á la Kalman filtering for metrology tool with application to coordinate measuring machines, at press in IEEE Trans. Ind. Electron., doi: 10.1109/TIE.2011.2162212, 2011.

[7] G. E. D'Errico and N. Murru, An algorithm for concurrent estimation of time-variant quantities, Meas. Sci. Technol., vol. 23, no. 045008 (9pp), doi: 10.1088/0957-0233/23/4/045008, 2012.

[8] R. K. Mehra, On the identification of variances and adaptive Kalman filtering, IEEE Trans. on Autom. Control, vol. AC–15, no. 2, pp. 175–184, 1970.

[9] K. A. Myers and B. D. Tapley, Adaptive sequential estimation with unknown noise statistics, IEEE Trans. Autom. Control, vol. **21**, no. **4**, pp. 520–523, 1976.

[10] B. J. Odelson, M. R. Rajamani, and J. B. Rawlings, A new autocovariance least–squares method for estimating noise covariances, Automatica, vol. 42, pp. 303–308, 2006.

[11] G. E. D'Errico, Paradigms for uncertainty treatments: a comparative analysis with application to measurement, Measurement, vol. 42, n. 4, pp. 494–500, 2009.

[12] Z. M. Durovic and B. D. Kovacevic, Robust estimation with unknown noise statistics, IEEE Trans. Autom. Control, vol. 44, no. 6, pp. 1292–1296, 1999.

[13] G. E. D'Errico and N. Murru, Fuzzy treatment of candidate outliers in measurements, Advances in Fuzzy Systems, Volume 2012, Article ID 783843 (6pp), doi: 10.1155/2012/783843, 2012.

[14] R. B. Nelsen, An introduction to copulas, 2nd edition, Springer, New York, 2007.

[15] BIPM, IEC, IFCC, ISO, IUPAC, IUPAP, and OIML, Evaluation of measurement data–Guide to the expression of uncertainty in measurement (GUM 1995 with minor corrections), JCGM 100: 2008.

[16] ASTM E178-08, Standard practice for dealing with outlying observations, American Society for Testing and Materials, 2008.

[17] G. E. D'Errico, Testing for outliers based on Bayes rule, Proc. XIX IMEKO World Congress on Fundamental and Applied Metrology, Sept. 6–11, 2009, Lisbon, Portugal.

[18] G. E. D'Errico, Issues in significance testing, Measurement, vol. 42, no. 10, pp. 1478-1481, 2009.

[19] BIPM, IEC, IFCC, ISO, IUPAC, IUPAP, and OIML, Evaluation of measurement data–Supplement 1 to the 'Guide to the expression of uncertainty in measurement'–Propagation of distributions using a Monte Carlo method JCGM 101: 2008.

[20] L. A. Zadeh, Fuzzy sets, Information and Control, vol. 8, 338–353, 1965.

[21] E. H. Mamdani and S. Assilian, An experiment in linguistic synthesis with a fuzzy logic controller, Int. J. of Man–Machine Studies, vol. 7, no. 1, 1–13, 1975.